PHYSICAL REVIEW B VOLUME 33, NUMBER 7 1 APRIL 1986

Critical behavior of coupled XY models

Enzo Granato* and J. M. Kosterlitz
Department of Physics, Brown University, Providence, Rhode Island 02912
(Received 30 September 1985)

Renormalization-group analysis is employed to investigate the critical behavior of coupled XY models. Recursion relations for small vortex fugacities and Migdal recursion relations in the strong-coupling limit are used to obtain the phase diagram. Several distinct phases are possible, separated by an XY-like and a p-state clocklike transition ($p=2,3$). The results are relevant for a number of systems that can be mapped onto coupled XY models.

I. INTRODUCTION

There has been much interest in two-dimensional classical XY models where the ground states exhibit both continuous and discrete degeneracy simultaneously. Among such systems one can mention the fully frustrated XY model,[1–3] which can be realized by a Josephson junction array in a transverse magnetic field with half a flux quantum per plaquette; the antiferromagnetic XY model on a triangular lattice;[4] the double-layer XY model[5] and the helical XY model.[6] From general symmetry arguments[3,7] or by using a Hubbard-Stratonovich transformation,[2] one expects that the phase transition in these systems can be analyzed by studying the critical behavior of coupled XY models described by the action

$$\begin{aligned} A = -H/k_BT = \alpha \sum_{\langle rr' \rangle} \cos[\theta(r)-\theta(r')] \\ +\beta \sum_{\langle rr' \rangle} \cos[\phi(r)-\phi(r')] \\ +h \sum_{r} \cos p[\theta(r)-\phi(r)] \, , \end{aligned} \tag{1.1}$$

where p is an integer and $\theta(r),\phi(r)$ are phases defined at the sites $r=(ma,na)$ of a square lattice with lattice spacing a.

The model has been analyzed previously for $p=1$ and $p=2$.[5,6] More recently, it has also been studied in Ref. 7. The analyses, however, were performed along the line $\alpha=\beta$ of initial coupling parameters.

In this paper we study the phase transition in coupled XY models using renormalization-group arguments. We analyze this model for $p=2$ and $p=3$ and $\alpha\neq\beta$ using an electrodynamic representation and derive the recursion relations for small vortex fugacities as well as Migdal recursion relations in the limit $h\to\infty$. Figure 2 shows the resulting phase diagram. The line APB corresponds to an Ising ($p=2$) or a 3-state Potts ($p=3$) transition. If the initial points of the Hamiltonian are along the line $\alpha=\beta$ a single transition occurs separating a locked phase with XY and Ising ($p=2$) order from a high-temperature XY and Ising disordered phase. The transition is a complicated point which we predict to be tetracritical in an as yet undetermined universality class. Further work needs to be done to determine this class for $p=2$ or $p=3$ although there are some intriguing indications from the numerical work[1,4,8] that this point may have simultaneous Ising and XY-like behavior.

The model with $\alpha\neq\beta$ has no experimental realization known to the authors except for $p=6$ when a slight modification describes a smectic C liquid-crystal film,[9] where one angle describes the projection of the molecule into the plane and the other the bond angle. It does however describe a frustrated XY magnet on a square lattice in which the strength of the antiferromagnetic and ferromagnetic bonds are not equal.[8]

Unfortunately our analyses cannot determine the behavior of the system on the $\alpha=\beta$ line except for arguments which are fairly conclusive that there is a single transition directly from a locked to disordered phase with no intervening phase with partial order. Also, it cannot unambiguously determine whether the transition from the locked to disordered phase for $\alpha\cong\beta$ is a single transition or a double transition with an intervening unlocked phase with algebraic order in one of the phase and disorder in the other. We incline to the view that there is such an unlocked phase in a region of the (α,β) plane except for a multicritical point on the $\alpha=\beta$ line. Thus we predict that such systems as the Josephson junction array on a square or triangular lattice with half a flux quantum per plaquette, the triangular XY antiferromagnet in zero magnetic field and the fully frustrated XY model on a square lattice, all have a single transition from the completely ordered to completely disordered phase. The analysis for the corresponding Ginsburg-Landau action in $4-\epsilon$ dimensions gives a first-order transition.[10] The mathematical model with $\alpha\neq\beta$ has a double transition, with an XY transition to a state of partial order followed by a transition in the p-state universality class to the locked phase.

Another model with similar but simpler properties is an XY model with interactions of different but commensurate periodicities.

$$A=\alpha \sum_{\langle rr' \rangle} \cos[\theta(r)-\theta(r')]+\beta \sum_{\langle rr' \rangle} \cos p[\theta(r)-\theta(r')] \, , \tag{1.2}$$

where the second term has periodicity $\theta\to\theta+2\pi/p$. This can be generalized to a similar model to that discussed previously by introducing two angles and a coupling term:

$$A=\alpha\sum_{\langle rr'\rangle}\cos[\theta(r)-\theta(r')]+\beta\sum_{\langle rr'\rangle}\cos[\phi(r)-\phi(r')]+h\sum_{r}\cos[p\theta(r)-\phi(r)]\ . \tag{1.3}$$

Figure 3 shows the resulting phase diagram. The model defined by (1.2) has also been studied recently in Ref. 11, using a different analysis.

This model may be related to fluid layers of liquid crystal where the molecules make a constant angle θ, ϕ relative to the normal to the plane. Then the local director is given by $n(r)=[\sin\phi\cos\theta(r),\sin\phi\sin\theta(r),\cos\phi]$. When the angle $\phi=\pi/2$, the molecules lie in the plane and the periodicity $\theta\to\theta+\pi$ must be observed. When they are not in the plane, θ and $\theta+\pi$ are no longer equivalent and a possible action describing this is

$$\begin{aligned}A&=-K\sum_{\alpha,\beta}\sum_{\langle rr'\rangle}[n^{\alpha}(r)n^{\beta}(r)-n^{\alpha}(r')n^{\beta}(r')]^2\\&=\text{const}+K\sin^2\phi\sum_{\langle rr'\rangle}\{4\cos^2\phi\cos[\theta(r)-\theta(r')]+\sin^2\phi\cos2[\theta(r)-\theta(r')]\}\ ,\end{aligned}$$

which has the correct limit when $\phi=\pi/2$ and describes a nematic. Depending on the tilt angle ϕ, the transition smectic $\leftrightarrow$ isotropic will take place either directly via an XY transition or through an intermediate nematic (unlocked) phase with an XY followed by an Ising transition as the temperature is lowered. This ignores the possibility of crystallization which may preempt one or both transitions. Unfortunately there is no experimental realization of a two-dimensional nematic because of rupturing of the film.

II. ELECTRODYNAMIC REPRESENTATION FOR COUPLED XY MODELS

In order to proceed with the investigation of the critical behavior in the model (1.1), we need to treat vortex excitations explicitly. This can be achieved by transforming the model to an equivalent electrodynamic representation.

First we write the symmetry breaking term as

$$\exp[h\cos p(\theta(r)-\phi(r))]=\sum_{S(r)}\exp\{ipS(r)[\theta(r)-\phi(r)]+\ln y_sS^2(r)\}\ . \tag{2.1}$$

If $y_s\to0$, only the terms $S=0$ and $S=\mp1$ contribute and the left- and right-hand side of (2.1) are equal provided $y_s=h/2$. When $y_s\to1$, $\theta(r)-\phi(r)$ is forced to take the values

$$(2\pi/p)\tau(r),\quad \tau(r)=0,1,2,\ldots,p-1\ . \tag{2.2}$$

Using the Villain approximation[12] for the first two cosine terms in (1.1), we consider the following partition function:

$$Z=\left[\prod_r\int_0^{2\pi}d\theta(r)\int_0^{2\pi}d\phi(r)\sum_{S(r)}\right]\times\left[\prod_{\langle rr'\rangle}\sum_{m(r,r')}\sum_{n(r,r')}\right]e^{A}\ , \tag{2.3}$$

where

$$\begin{aligned}A=&-\frac{\alpha}{2}\sum_{\langle rr'\rangle}[\theta(r)-\theta(r')-2\pi m(r,r')]^2-g\sum_{\langle rr'\rangle}[\theta(r)-\theta(r')-2\pi m(r,r')][\phi(r)-\phi(r')-2\pi n(r,r')]\\&-\frac{\beta}{2}\sum_{\langle rr'\rangle}[\phi(r)-\phi(r')-2\pi n(r,r')]^2+ip\sum_r S(r)[\theta(r)-\phi(r)]\ .\end{aligned} \tag{2.4}$$

The additional coupling parameter g is introduced above because it is generated by the renormalization procedure that we shall use. Following Kadanoff,[13] we introduce integer valued variables $M(R)=\oint m(r,r')$ and $N(R)=\oint n(r,r')$ defined on the sites R of the dual lattice, so that $N(R)$ and $M(R)$ are regarded as vortex variables associated with the fields $\theta(r)$ and $\phi(r)$ respectively. The symbol $\oint$ indicates a discrete curl around the dual site R.

With these definitions it is found that the equivalent electrodynamic representation of (1.1) is

$$Z=\left[\prod_r\sum_{S(r)}{}'\right]\left[\prod_R\sum_{M(R)}{}'\sum_{N(R)}{}'\right]e^{A(M,N,S)}\ , \tag{2.5}$$

where

$$\begin{aligned}A(M,N,S)=&\pi\alpha\sum_{R,R'}M(R)G(R-R')M(R')+\pi\beta\sum_{R,R'}N(R)G(R-R')N(R')\\&+2\pi g\sum_{R,R'}M(R)G(R-R')N(R')+pi\sum_r\sum_R S(r)\Theta(r-R)[M(R)-N(R)]+\pi\gamma\sum_{r,r'}S(r)G(r-r')S(r')\end{aligned} \tag{2.6}$$

and

$$\gamma=\frac{p^2(\alpha+\beta+2g)}{4\pi^2(\alpha\beta-g^2)}\ . \tag{2.7}$$

The primes on the summations over the three integer fields indicate that they are subject to the neutrality condition

$$\sum_R M(R)=\sum_R N(R)=\sum_r S(r)=0 \ . \tag{2.8}$$

The large-distance behavior of the Green's functions $G(R-R')$ and $\Theta(r-R)$ are

$$\begin{aligned} G(R-R')&=\ln(|R-R'|/a)+\pi/2 \ , \\ \Theta(r)&=\tan^{-1}(y/x) \ , \end{aligned} \tag{2.9}$$

where $r=(x,y)$. Correlations functions can be treated similarly. We find, for large displacements $|\rho-\rho'|$,

$$\begin{aligned} \langle \exp iq(\theta(\rho)-\theta(\rho'))\rangle = |\rho-\rho'|^{-q^2\beta/2\pi(\alpha\beta-g^2)}Z^{-1}\left[\prod_r \sum_{S(r)}{}'\right]\left[\prod_R \sum_{M(R)}{}' \sum_{N(R)}{}'\right]\exp A(M,N,S) \\ \times\exp\left[iq\sum_R M(R)[\Theta(\rho-R)-\Theta(\rho'-R)]+\frac{qp(\beta+g)}{2\pi(\alpha\beta-g^2)}\sum_r S(r)[G(r-\rho)-G(r-\rho')]\right] \ , \end{aligned} \tag{2.10}$$

$$\begin{aligned} \langle \exp iq(\phi(\rho)-\phi(\rho'))\rangle = |\rho-\rho'|^{-q^2\alpha/2\pi(\alpha\beta-g^2)}Z^{-1}\left[\prod_r \sum_{S(r)}{}'\right]\left[\prod_R \sum_{M(R)}{}' \sum_{N(R)}{}'\right]\exp A(M,N,S) \\ \times\exp\left[iq\sum_R N(R)[\Theta(\rho-R)-\Theta(\rho'-R)]-\frac{qp(\alpha+g)}{2\pi(\alpha\beta-g^2)}\sum_r S(r)[G(r-\rho)-G(r-\rho')]\right] \ , \end{aligned} \tag{2.11}$$

$$\begin{aligned} \langle \exp iq(\theta(\rho)-\phi(\rho'))\rangle = |\rho-\rho'|^{q^2 g/2\pi(\alpha\beta-g^2)}e^{q^2(\alpha+\beta+2g)/8(\alpha\beta-g^2)}Z^{-1}\left[\prod_r \sum_{S(r)}{}'\right]\left[\prod_R \sum_{M(R)}{}' \sum_{N(R)}{}'\right]\exp A(M,N,S) \\ \times\exp\Bigg[iq\sum_R M(R)\Theta(\rho-R)-iq\sum_R N(R)\Theta(\rho'-R) \\ +\frac{qp}{2\pi(\alpha\beta-g^2)}\sum_r S(r)[(\beta+g)G(r-\rho)+(\alpha+g)G(r-\rho')]\Bigg] \ , \end{aligned} \tag{2.12}$$

for integer values of q.

III. RECURSION RELATIONS IN THE WEAK-COUPLING LIMIT

In order to remove the short-ranged interactions from the representation (2.6), we shall extend the renormalization-group method for the XY model.[14] The $|R-R'|=a$ and $|r-r'|=a$ terms in (2.6) generate the followings terms:

$$\sum_R M^2(R)\ln y_m+\sum_R N^2(R)\ln y_n+\sum_r S^2(r)\ln y_s \ ,$$

where

$$\begin{aligned} y_m&=\exp(-\pi^2\alpha/2) \ , \\ y_n&=\exp(-\pi^2\beta/2) \ , \\ y_s&=(h/2)\exp(-\pi^2\gamma/2) \end{aligned} \tag{3.1}$$

are the fugacities for their respective charges. There is an additional term $\pi^2 g\sum_R M(R)N(R)$ that can provide a fugacity associated to hybrid vortices, i.e., configurations in which M vortex and N vortex reside at the same site. The resulting recursion relations are discussed in the Appendix. In order to restrict the charges to take only the values 0 and ±1, we consider only small values of the fugacities. The effect of small y_s is to unlock the variables $\theta(r)$ and $\phi(r)$ in the partition function (1.1) and corresponds to h small.

The recursion relations for the fugacities are ($dl=da/a$),

$$\begin{aligned} \frac{dy_m}{dl}&=(2-\pi\alpha)y_m \ , \\ \frac{dy_n}{dl}&=(2-\pi\beta)y_n \ , \\ \frac{dy_s}{dl}&=(2-\pi\gamma)y_s \ . \end{aligned} \tag{3.2}$$

The coefficient α is renormalized by considering all contributions from the rescaling of the lattice spacing $a\to a+da$ which are proportional to MGM. These contributions are

$$\begin{aligned} &(2\pi\alpha)^2 MG\overline{MM}GM \ , \\ &(2\pi g)^2 MG\overline{NN}GM \ , \\ &(-ip)^2 M\Theta\overline{SS}\Theta M \ . \end{aligned} \tag{3.3}$$

The last term presents no special problems since one can make use of the property $(\nabla G)^2=(\nabla\Theta)^2$. For the other coefficients the procedure is the same. The corresponding recursion relations are

$$\begin{aligned}\frac{d\alpha}{dl}&=-4\pi^3\alpha^2y_m^2-4\pi^3g^2y_n^2+\pi p^2y_s^2\ ,\\ \frac{dg}{dl}&=-4\pi^3\alpha g y_m^2-4\pi^3\beta g y_n^2-\pi p^2y_s^2\ ,\\ \frac{d\beta}{dl}&=-4\pi^3\beta^2y_n^2-4\pi^3g^2y_m^2+\pi p^2y_s^2\ ,\\ \frac{d\gamma}{dl}&=-4\pi^3\gamma^2y_s^2+\pi p^2y_m^2+\pi p^2y_n^2\ .\end{aligned}\tag{3.4}$$

Using Eq. (2.7) one finds that the recursion relation for γ is consistent with the other three and therefore is redundant.

By considering the region of the (α,g,β) parameter space for which $\pi\beta>2$ and using Eqs. (3.2), it is apparent that the fugacity y_n is irrelevant in this region. This irrelevance allows us to consider $N(R)=0$ in (2.6). A numerical iteration of (3.4) shows that there is a region in which y_n is irrelevant. The action is consequently simplified to

$$\begin{aligned}A(M,S)=\pi\alpha&\sum_{R,R'}M(R)G(R-R')M(R')\\&+pi\sum_r\sum_R S(r)\Theta(r-R)M(R)\\&+\frac{p^2(\alpha+\beta+2g)}{4\pi(\alpha\beta-g^2)}\sum_{r,r'}S(r)G(r-r')S(r')\ .\end{aligned}\tag{3.5}$$

It is now possible to exploit the dual symmetry[13] of this action under the transformation $M\leftrightarrow S$. Provided one chooses $y_m=y_s$, there is a self-dual surface in the (α,g,β) parameter space given by

$$4\pi^2\alpha(\alpha\beta-g^2)=p^2(\alpha+\beta+2g)\ .\tag{3.6}$$

For $p=2$ and $p=3$ this must represent the boundary between two low-temperature phases. The renormalization-group recursion relations (3.2) and (3.4) on the self-dual surface $y_m=y_s=y$ now reads

$$\begin{aligned}\frac{dy}{dl}&=(2-\pi\alpha)y\ ,\\ \frac{d\alpha}{dl}&=4\pi y^2(p^2/4-\pi^2\alpha^2)\ ,\\ \frac{dg}{dl}&=-4\pi y^2(p^2/4+\pi^2\alpha g)\ ,\\ \frac{d\beta}{dl}&=4\pi y^2(p^2/4-\pi^2g^2)\ .\end{aligned}\tag{3.7}$$

It is clear from these equations that $\pi\alpha$ will decrease from an initial value greater than $p/2$. It must eventually flow to a line of attractive fixed points somewhere else in the self-dual surface. Assuming that Eqs. (3.7) are qualitatively true for all values of y, it can be speculated that these fixed points occur for $\pi\alpha=p/2$ and $\pi g=-p/2$ with $y\cong1$, independent of β. Therefore the renormalized action must be characterized by a surface in the (α,g,β) parameter space, intersecting the self-dual surface along the line $\pi\alpha=p/2$, $\pi g=-p/2$ with $y_m=y_s\cong1$.

From Eqs. (3.4), with $y_n=0$, it is found that

$$\frac{d}{dl}(\alpha+g)=-4\pi^3\alpha(\alpha+g)y_m^2\ .\tag{3.8}$$

This suggests that this surface is given by $\alpha+g=0$ with $y_m=y_s\cong1$, in the vicinity of the fixed points.

Using $\alpha+g=0$ in (2.7), we have $\pi\gamma=p^2/4\pi\alpha$ and the action (2.6) with $N(R)=0$ reduces to

$$\begin{aligned}A(M,S)=\pi\alpha&\sum_{R,R'}M(R)G(R-R')M(R')\\&+pi\sum_r\sum_R S(r)\Theta(r-R)M(R)\\&+\frac{p^2}{4\pi\alpha}\sum_{r,r'}S(r)G(r-r')S(r')\ ,\end{aligned}\tag{3.9}$$

which is recognizable as that of a p-state clock model.[15] This indicates that the phase transition is governed by a line of fixed points of Ising character ($p=2$) or 3-state Potts character ($p=3$). The same analysis can be performed for the region of the parameter space $\pi\alpha>2$. By symmetry we then obtain another line of fixed points at $\pi\beta=p/2$ and $y_n=y_s\cong1$.

In addition to those lines of fixed points we also expect two lines of fixed points along the axis for $\alpha=0$, $\pi\beta>2$, and $\beta=0$, and $\pi\alpha>2$ corresponding to the usual XY line of fixed points for a single XY model. In the limit $\beta\to\infty$, (1.1) reduces to an XY model with symmetry breaking field,[16] one then expects an Ising-like and a 3-state-Potts–like transition for $p=2$ and $p=3$, respectively. For α near zero, the M vortices are highly relevant and can be integrated out. This procedure leads to an effective $\beta_{\rm eff}=\beta-g^2/\alpha$ and the S variables bound together by strings with a linear interaction and therefore irrelevant (see the discussion in Sec. V). So the transition temperature at finite g should be decreased. The expected pattern of renormalization-group trajectories is indicated in Fig. 1.

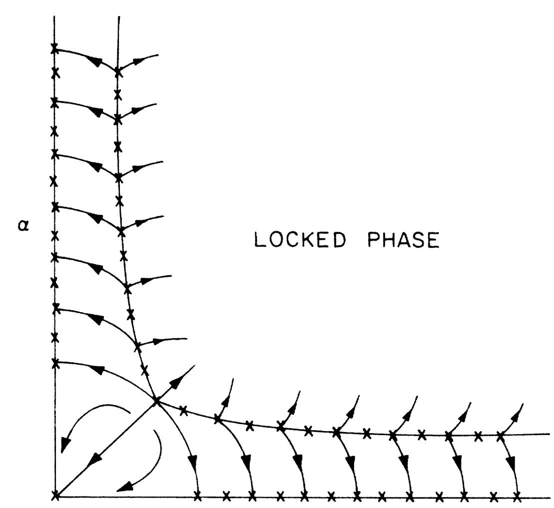

FIG. 1. Schematic renormalization-group trajectories.

A numerical iteration of Eqs. (3.4) performed until the fugacities are of order 1, confirms Fig. 1 and gives the phase diagram of Fig. 2. A distinct point P along the line of initial points $\alpha=\beta$ separates the low- and the high-temperature phases. The locked phase corresponds to a power-law decay of correlations for $\theta(r)$ and $\phi(r)$ fields, and in this region, fluctuations in $\theta(r)$ are tied to fluctuations in $\phi(r)$. Phase B corresponds to Ising-like ($p=2$) or 3-state-Potts—like ($p=3$) disorder and XY-like order in the field $\phi(r)$ and it is separated from the locked phase by an Ising (or 3-state Potts) line PB. Phase A corresponds to the analogous behavior for the field $\theta(r)$. Both phases in turn are separated from the high-temperature phase corresponding to Ising (3-states Potts) disorder and XY disorder by the line CPD. We are unable to determine in which form the two lines meet at the point P.

The difference between our model and the p-state clock model transition along the line APB lies in the behavior of the correlation functions. If $\alpha+g=0$ and $N(R)=0$ the expression (2.10) reduces to

$$\langle \exp[iq(\theta(\rho)-\theta(\rho'))]\rangle = |\rho-\rho'|^{-q^2\eta}F_p^q(\rho-\rho') . \quad (3.10)$$

Here $F_p^q(\rho-\rho')$ is the corresponding correlation function for the p-state clock model[15] with $F_p^p=1$ and

$$\eta=1/2\pi(\beta-\alpha) . \quad (3.11)$$

for the field $\phi(r)$ we similarly find

$$\langle \exp[iq(\phi(\rho)-\phi(\rho'))]\rangle = |\rho-\rho'|^{-q^2\eta} . \quad (3.12)$$

Near the line PB the correlation function $F_p^{q=1}(\rho-\rho')$ approaches a constant or decays exponentially to zero as $|\rho-\rho'|\to\infty$ if we are above or below this line, respectively. It follows that for phase A,

$$\langle \exp[i(\theta(\rho)-\theta(\rho')]\rangle = |\rho-\rho'|^{-\eta_A(\alpha,g,\beta)} ,$$

$$\langle \exp[i(\phi(\rho)-\phi(\rho'))]\rangle = |\rho-\rho'|^{-\eta_A(\alpha,g,\beta)}e^{-|\rho-\rho'|/\xi} ,$$

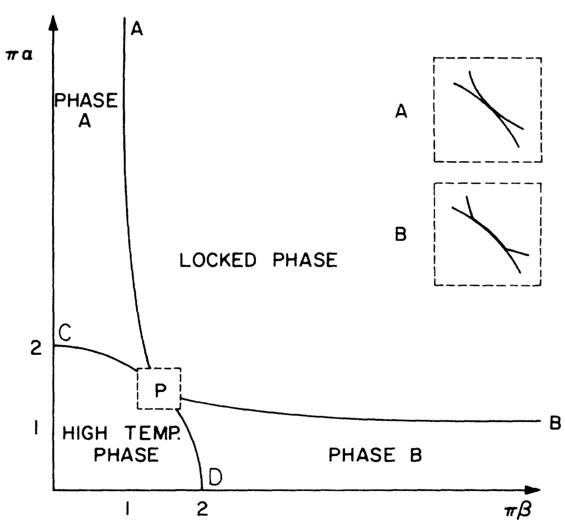

FIG. 2. Topological features of the phase diagram. The manner the lines merge at P is not determined. Two possibilities are indicated in the insets A and B. Phases A and B are partial ordered unlocked phases.

where ξ is the correlation length of the p-state clock model. Similarly, for phase B,

$$\langle \exp[i(\phi(\rho)-\phi(\rho'))]\rangle = |\rho-\rho'|^{-\eta_B(\alpha,g,\beta)} ,$$

$$\langle \exp[i(\theta(\rho)-\theta(\rho'))]\rangle = |\rho-\rho'|^{-\eta_B(\alpha,g,\beta)}e^{-|\rho-\rho'|/\xi} .$$

Note that for $q=p$, all correlation functions are algebraic in all ordered phases. In the high temperature phase all correlation functions decay exponentially.

In the region where $\pi\alpha>2$ and $\pi\beta>2$ we can take $M(R),N(R)=0$. In this region $S(r)$ is relevant. Nevertheless, one can transform (2.10) and (2.11) to another representation with the corresponding integer fields dilute in that regime. Using the Poisson summation formula,

$$\sum_s g(s)=\sum_h \int_{-\infty}^{\infty} d\phi g(\phi)e^{-2\pi ih\phi} , \quad (3.13)$$

after integrating over the continuous field introduced by (3.13), the correlation functions (2.10) and (2.11) factorize into a power-law term times the corresponding correlation function for the roughening model in the low-temperature regime. Since one expects that this correlation function will tend to a nonzero value as $|\rho-\rho'|\to\infty$, we obtain

$$\begin{aligned}\langle \exp[iq(\theta(\rho)-\theta(\rho'))]\rangle &= |\rho-\rho'|^{-q^2\eta} ,\\ \langle \exp[iq(\phi(\rho)-\phi(\rho'))]\rangle &= |\rho-\rho'|^{-q^2\eta} ,\end{aligned} \quad (3.14)$$

and

$$\langle \exp[iq(\theta(\rho)-\phi(\rho'))]\rangle = |\rho-\rho'|^{-q^2\eta} , \quad (3.15)$$

with $\eta=1/2\pi(\alpha+\beta+2g)$

Therefore in this region these correlations decay algebraically and are characterized by the same renormalized constant (3.15) and the corresponding phase is locked. Although this analysis was performed for the region $\pi\alpha>2$ and $\pi\beta>2$, the Migdal renormalization-group analysis to be discussed later, suggests that the low-temperature side of the line APB is all locked and the behavior described by (3.14) and (3.15) extends throughout the region. In the unlocked phases A and B standard arguments imply that $0<\eta_{A,B}<\frac{1}{4}$, the upper value being reached on the phase boundaries between the partially ordered and completely disordered phases.

IV. STRONG-COUPLING LIMIT AND THE MIGDAL RECURSION RELATIONS

The analysis of the preceding section shows that in the locked phase, y_s is relevant; this corresponds to $h\to\infty$ in (2.1). In this limit $\theta(r)-\phi(r)$ assumes the values given by (2.2). For $p=2$ one can define the Ising variables $S(r)=2\tau(r)-1$ and obtain[2]

$$A=\beta\sum_{\langle rr'\rangle}\cos[\phi(r)-\phi(r')] + \alpha\sum_{\langle rr'\rangle}S(r)S(r')\cos[\phi(r)-\phi(r')] . \quad (4.1)$$

This action will describe the critical behavior associated to the field $\phi(r)$. We can investigate the phase diagram of this model by using the approximate position-space renormalization-group transformation introduced by Migdal.[17] Here we apply this transformation in a form due to Kadanoff.[18]

First we need to consider a more general form of the action (4.1):

$$A=\sum_{\langle rr'\rangle} V(\phi(r)-\phi(r')) + \sum_{\langle rr'\rangle} S(r)S(r')F(\phi(r)-\phi(r')) + L\sum_{\langle rr'\rangle} S(r)S(r') , \quad (4.2)$$

where $V(\phi)$ and $F(\phi)$ are periodic functions with period 2π. The original expression (4.1) is recovered upon setting $V(\phi)=\beta\cos\phi$, $F(\phi)=\alpha\cos\phi$, and $L=0$. The additional term has to be included since the form (4.1) is not preserved under renormalization. To apply the Migdal transformation one first moves bonds on the lattice such that the sites to be integrated out at each stage are linked to their neighbors only in one spacial direction. This bond moving allows us to perform a one-dimensional decimation to obtain an effective interaction between the remaining degrees of freedom. In terms of $u(\phi)=\exp[V(\phi)-V(0)]$, $z=\exp[F(0)+L]$, and $f(\phi)=\exp[F(\phi)-F(0)]$ the parameters (primed) of the new Hamiltonian are therefore given by the recursion relations:

$$(z')^2=\frac{z^4A_1(0)+z^{-4}A_4(0)}{A_2(0)+A_3(0)} ,$$

$$(u')^2(\phi)=\frac{[A_2(\phi)+A_3(\phi)][z^4A_1(\phi)+z^{-4}A_4(\phi)]}{[A_2(0)+A_3(0)][z^4A_1(0)+z^{-4}A_4(0)]} , \quad (4.3)$$

$$(f')^2(\phi)=\frac{[A_2(0)+A_3(0)][z^4A_1(\phi)+z^{-4}A_4(\phi)]}{[z^4A_1(0)+z^{-4}A_4(0)][A_2(\phi)+A_3(\phi)]} ,$$

where

$$A_1(\phi)=\int_0^{2\pi}\frac{d\theta}{2\pi}u^2(\theta)u^2(\theta-\phi)f^2(\theta)f^2(\theta-\phi) ,$$

$$A_2(\phi)=\int_0^{2\pi}\frac{d\theta}{2\pi}u^2(\theta)u^2(\theta-\phi)f^{-2}(\theta)f^2(\theta-\phi) ,$$

$$A_3(\phi)=\int_0^{2\pi}\frac{d\theta}{2\pi}u^2(\theta)u^2(\theta-\phi)f^2(\theta)f^{-2}(\theta-\phi) , \quad (4.4)$$

$$A_4(\phi)=\int_0^{2\pi}\frac{d\theta}{2\pi}u^2(\theta)u^2(\theta-\phi)f^{-2}(\theta)f^{-2}(\theta-\phi) .$$

A numerical iteration of Eqs. (4.3) gives a phase diagram similar to Fig. 2. The line APB separates the low-temperature region where $L\to\infty$ (Ising order) from the regions B and A where $L\to 0$ (Ising disorder). In this figure the axial parameters are now defined by $\alpha_{\rm eff}=(-\frac{1}{2})\ln f(\pi)$ and $\beta_{\rm eff}=(-\frac{1}{2})\ln u(\pi)$. They reduce to α and β, respectively, for the initial values $u(\phi)=e^{\beta\cos\phi-\beta}$ and $f(\phi)=e^{\alpha\cos\phi-\alpha}$. Actually, one should observe the evolution of the functions $u(\phi)$ and $f(\phi)$ in the whole interval $0\le\phi\le 2\pi$, but the above defined parameters provide a convenient way of following the renormalization flows. Above and below the line PB, after a few iterations, $f(\phi)\to 1$ and $u(\phi)$ relaxes to a Villain potential.[12] Unfortunately the Migdal transformation does not actually lead to a fixed line and a small drift toward higher temperatures is always present.[16] Therefore the line CD separating the disordered high-temperature phase from the fixed line $\beta>\beta_D$ cannot be precisely determined.

The line APB corresponds to Ising-like transition. In fact for $\beta>\alpha$, $f(\phi)$ and $u(\phi)$ renormalize to $f'(\phi)=1$ and $u'(\phi)=u^*(\phi)$. Using the recursion relations (4.3) we find $\delta L'=e^{\lambda\ln 2}\delta L$, where $\delta L'$ and δL are the deviations from the fixed point and $\lambda=0.74$. This is the same result one finds for the two-dimensional Ising model using the same approximation.

Near the point P, however, we cannot estimate the critical exponents due to the drift to high temperatures in the Migdal approximation. Again we cannot determine the way the two lines join or the kind of transition at that particular point. It is apparently consistent with a single transition but if two successive transitions do in fact occur the Migdal approximation then indicates they are very close together with an XY transition followed by an Ising transition as temperature is increased. In particular we find that the region above the Ising line PB is a locked phase with power-law decay of correlations. Although we have studied the limit $h\to\infty$ for the case $p=2$, we also expect similar results for $p=3$, where instead of an Ising we would have a 3-state Potts transition.[2]

V. LINEAR AND LOGARITHMIC INTERACTING VORTICES

In the model (1.1), vortex excitations can appear as a result of the continuous symmetry of the action in both $\theta(r)$ and $\phi(r)$ fields. Not all the ground states can be connected by a continuous transformation and the ground state has a discrete degeneracy. A domain wall excitation therefore separates a ground-state configuration corresponding to $\theta(r)-\phi(r)=0$ from another nonequivalent ground state $\theta(r)-\phi(r)=2\pi/p$.

The energy of an isolated vortex is proportional to $\ln L$, where L is the linear dimension of the system. Therefore one expects logarithmic interacting vortex pairs of opposite vorticities at low temperatures. Since the entropy of such a pair is also proportional to $\ln L$, they can unbind at some higher temperature.

On the other hand, since there is a change of phase of $2\pi/p$ when crossing a domain wall, one can also produce a vortex by joining to the same point the ends of p domain walls.[19] The energy of such a vortex is proportional to the linear dimension of the system because a domain wall has a finite energy per unit length. Therefore, at low temperatures one expects they are connected by strings (domain walls) in pairs of opposite vorticities. This linear interaction suppresses an XY-like unbinding.

In the locked phase y_s is strongly relevant. One can now transform (2.6) into another representation where the corresponding integer fields are dilute in that regime using (3.13) again. The necessary manipulations are essentially the same as described in Ref. 20. Dropping an overall constant factor, we get

$$Z=\left[\prod_{R}\sum_{M(R)}{}'\sum_{N(R)}{}'\right]e^{A(M,N)}\,, \tag{5.1}$$

where

$$\begin{aligned}e^{A(M,N)}=\exp\Bigg[&\pi(\alpha-p^2/4\pi^2\gamma)\sum_{R,R'}M(R)G(R-R')M(R')+\pi(\beta-p^2/4\pi^2\gamma)\sum_{R,R'}N(R)G(R-R')N(R')\\&+2\pi(g+p^2/4\pi^2\gamma)\sum_{R,R'}M(R)G(R-R')N(R')\Bigg]\\&\times\left[\prod_{r}\sum_{h(r)}\right]\exp\left[-(1/2\gamma)\sum_{\langle rr'\rangle}\left[h(r)-h(r')-p\sum_{R}\eta_{rr'}(R)[M(R)-N(R)]\right]^2\right].\end{aligned} \tag{5.2}$$

$\eta_{rr'}(R)$ is the operator introduced in Ref. 16, it is $+1$ if r lies just to the right and r' just to the left of an arbitrary path going from R to ∞ in the positive x direction, -1 if r and r' are reversed, and 0 otherwise.

The first three terms in (5.2) represent logarithmic interacting vortices now corrected by a term $p^2/4\pi^2\gamma$ due to domain walls. The last term corresponds to the partition function for a set of domain walls of strength p running from R to R' in the roughening model.[21] Thus this term represents vortex pairs interacting linearly and connected by p domain walls of unit strength. The interaction energy for a vortex pair has therefore two contributions: a logarithmic and a linear distance dependence. If the strings have not melted these vortex pairs interact linearly for large distance separations and an XY-unbinding transition is suppressed. However when the strings melt these vortices interact logarithmically, as can be seen by replacing the sum of the integers $h(r)$ by an integral over a continuous field. The corresponding phase now depends on the behavior of these vortices. The $M(R)$ vortices would unbind for $\pi\alpha<2$ and the $N(R)$ for $\pi\beta<2$. If the melting of the domain walls occurs inside these regions the relevant vortex pair will unbind at that temperature and disorder the corresponding field.

From (5.2) we can identify the free energy per unit length (divided by k_BT) of a domain wall as $1/2\gamma$ when $T\to 0$. Using a Peierls argument to determine when the free energy of a domain wall goes to zero we obtain that the string melting occurs at temperatures given by $\gamma=1/2\ln 3$. This gives melting curves similar to APB in Fig. 2. When $g=0$, this curve intersects the region where $\pi\alpha<2$ and $\pi\beta<2$ only for $p=2$. However, the effect of a renormalized $g<0$ is to move these lines further inside that region. In particular, for $g=-\alpha$ along the line $\alpha=\beta$, the $p=3$ melting curve also intersects this region but $p=4$ curve does not. Thus we expect that for $p=2$ and $p=3$ there is no intermediate phase with XY order and p-state clock disorder ($p=2,3$) and we are left with the two possibilities indicated in Fig. 2.

On the $\alpha=\beta$ line, which is, of course, the most interesting from an experimental point of view, the weak coupling recursion relations do not say very much because one can construct a large number of relevant operators. In particular the M, N, and S charges are all relevant with increasing fugacities. Also, the hybrid vortices with $M(R)=N(R)$ on the same site are highly relevant, while the hybrid vortices with $M(R)=-N(R)$ are irrelevant and will be ignored. Now at large α the M, N, and H vortices are irrelevant but y_s is strongly relevant which when integrated out gives the string picture. When the temperature is increased (α decreased) although the recursion relations seem to indicate that the M and N vortices are relevant they are still bound together by strings. The hybrid vortices are not bound by strings [Eq. (5.2)]. So, the important configurations are: (i) a pair of $M(N)$ vortices of opposite signs bound by strings well separated from any $N(M)$ vortices; (ii) one M and one N vortex of the same sign close together bound by strings which can be regarded as a hybrid (H) vortex with a core size of the order of their separation.

These extended objects interact logarithmically with each other on length scales large compared to their size. The separation of the M and N of the same sign can be interpreted as the core size of a hybrid vortex. For $p=2$ and 3, simple estimates for the sequence of transition temperatures give $T_M<T_S<T_H$, where T_M is the unbinding temperature of M or N vortices, T_S is the string melting temperature, and T_H is the hybrid vortex unbinding temperature. The M vortices are bound by p strings so the transition in the absence of hybrid vortices would be in the p-state universality class by the string melting. However, the hybrid vortices are screened at $T>T_S$ by the M and N vortices so that they must unbind when the M and N do. Below T_S the M and N vortices are bound for separations less than ξ_p, the correlation length of the p-state model, which can be interpreted as the core size of a hybrid vortex. Thus, in the presence of hybrid vortices, the XY order is lost by the divergence of the hybrid vortex core size which leads one to expect a first-order transition. Note that this picture is fairly close to that described in Ref. 3, where it was derived on very physical grounds. Furthermore, this picture gives an explanation of the mixed p state and XY character of the system as one approaches the transition provided it is rather weakly first order.

These arguments can be applied to the same model with

$p=1$ which is the Villain representation of the double-layer XY model.[5] However the sequence of transition temperatures is $T_M < T_H < T_S$. So this scenario means that the M and N vortices remain bound by strings and the transition is controlled entirely by the hybrid vortices leading to the expected XY transition.

Unfortunately, there is no evidence for such a first-order transition from the extensive Monte Carlo simulations performed on this and related models[1,4,8] in 80×80 systems which indicate a transition of mixed Ising and XY character. However, because the unit cell in the triangular antiferromagnet is $\xi_0=\sqrt{3}a$ and in the frustrated XY model on the square lattice $2a$, the largest correlation length is about 30 unit cells long. So there is no sign of a first-order transition up to $\xi/\xi_0 \simeq 30$ and so the transition is at best weakly first order.

VI. COMPETING PERIODICITIES

In this section we will discuss the XY model with competing interactions described by Eq. (1.3) in the Villain approximation. A related model was discussed in Ref. 11. The electrodynamic representation of the action is found, by the methods of Sec. II, to be

$$Z=\left[\prod_r \sum_{S(r)}{}'\right]\left[\prod_R \sum_{M(R)}{}' \sum_{N(R)}{}'\right] e^{A(M,N,S)} ,$$

where

$$A(M,N,S)=\pi\alpha \sum_{R,R'} M(R)G(R-R')M(R')+\pi\beta \sum_{R,R'} N(R)G(R-R')N(R') + 2\pi g \sum_{R,R'} M(R)G(R-R')N(R')+i\sum_r \sum_R S(r)\Theta(r-R)[pM(R)-N(R)]+\pi\gamma \sum_{r,r'} S(r)G(r-r')S(r') , \tag{6.1}$$

where

$$\gamma=\frac{(\alpha+p^2\beta+2pg)}{4\pi^2(\alpha\beta-g^2)} . \tag{6.2}$$

The analysis is almost identical and we find a self-dual surface when the $N(R)$ vortices are irrelevant given by $\alpha=\gamma$ which corresponds to a p-state transition. The renormalization-group equations on this surface seem to flow to the fixed point at $\pi\alpha=p/2$ and $\pi g=-\frac{1}{2}$ independent of β. Identical arguments to Sec. V show that this is a string melting transition between the fully and partially ordered phases of Ref. 11. The other self-dual line at small values of β does not correspond to a phase transition since it is the XY model in a magnetic field. The phase diagram is sketched in Fig. 3 in which phase A is the locked phase and phase B is a partially ordered unlocked phase. The nature of the multicritical point P cannot be determined by these methods although applying the arguments of the previous section indicate that there is a first-order segment on the line CP in the neighborhood of P. Note that this p-state transition is not a consequence of an extra Z_p symmetry in the Hamiltonian, but simply due to extra minima in the action for $\alpha < 4\beta$.

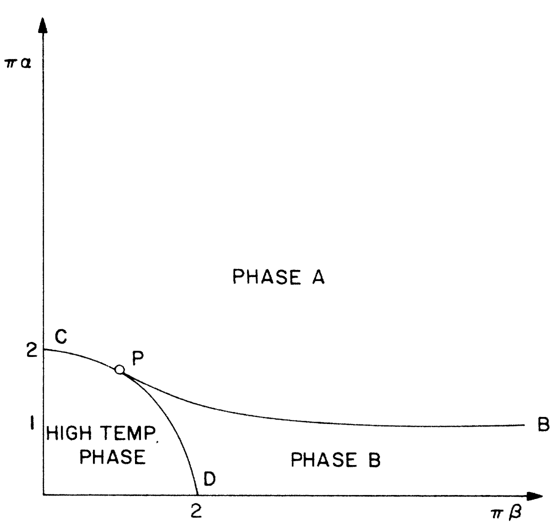

FIG. 3. Schematic phase diagram for an XY model with competing periodicities. Phase A is a locked phase and phase B is a partial ordered unlocked phase.

VII. CONCLUSIONS

We have investigated a class of coupled XY models with and without degenerate minima in the action by weak-coupling renormalization-group methods, approximate Migdal recursion relations and by qualitative arguments based on vortices and strings. A rich phase structure is found with several ordered and partially ordered phases. The universality classes for the transitions between ordered and partially ordered phases assuming them to be continuous is elucidated. The transitions from the locked fully ordered phase with long-range p state and algebraic XY order are argued to be single transitions in contrast to Miyashita and Shiba[4] and Garel and Doniach[6] and probably to be weakly first order. We have also argued that the observed simultaneous XY and p-state character of the transition found in Monte Carlo simulations[4,8] is obtained from the theoretical models.

However, the $\alpha=\beta$ line of the action of Eq. (1.1), which is the most interesting from the experimental point of view, is the least amenable to theoretical analysis. This with $p=2$ corresponds to Josephson junction arrays with half a flux quantum per plaquette and when accurate experimental determinations of the I-V characteristics become available it would be of great interest to compare them with theory. To do this, one would very much like to know what sort of transition one is dealing with but the methods used in this paper are not sufficiently powerful and this problem must be left to the future.

ACKNOWLEDGMENTS

E.G. was supported by the Conselho Nacional de Desenvolvimento Cientifico e Tecnológico (Brazil). J.M.K. was supported by National Science Foundation under Grant No. DMR-83-05022.

APPENDIX

We consider the recursion relations for (2.6) when hybrid vortices are also included. Only hybrid vortices in which an M vortex and an N vortex have the same sign are found to be relevant when $g<0$. We can rewrite (2.6) as

$$\begin{aligned}A=&\pi\alpha\sum_{R,R'}M(R)G(R-R')M(R')+\pi\beta\sum_{R,R'}N(R)G(R-R')N(R')+2\pi g\sum_{R,R'}M(R)G(R-R')N(R')\\&+ip\sum_{r}\sum_{R}S(r)\Theta(r-R)M(R)-ip\sum_{r}\sum_{R}S(r)\Theta(r-R)N(R)\\&+\pi\gamma\sum_{r,r'}S(r)G(r-r')S(r')+2\pi(\alpha+g)\sum_{R,R'}M(R)G(R-R')H(R')\\&+2\pi(\beta+g)\sum_{R,R'}N(R)G(R-R')H(R')+\pi(\alpha+\beta+2g)\sum_{R,R'}H(R)G(R-R')H(R')\ ,\end{aligned}\tag{A1}$$

where $H(R)$ is a hybrid vortex at site R and the summations over $M(R)$ and $N(R)$ exclude positions where they reside at the same site. Similarly to (3.2) and (3.4) we now obtain

$$\begin{aligned}\frac{dy_m}{dl}&=(2-\pi\alpha)y_m\ ,\\\frac{dy_n}{dl}&=(2-\pi\beta)y_n\ ,\\\frac{dy_s}{dl}&=(2-\pi\gamma)y_s\ ,\\\frac{dy_H}{dl}&=[2-\pi(\alpha+\beta+2g)]y_H\ ,\\\frac{d\alpha}{dl}&=-4\pi^3\alpha^2y_m^2-4\pi^3g^2y_n^2+\pi p^2y_s^2-4\pi^3(\alpha+g)^2y_H^2\ ,\\\frac{dg}{dl}&=-4\pi^3\alpha g y_m^2-4\pi^3\beta g y_n^2-\pi p^2y_s^2\\&\quad-4\pi^3(\alpha+g)(\beta+g)y_H^2\ ,\\\frac{d\beta}{dl}&=-4\pi^3\beta^2y_n^2-4\pi^3g^2y_m^2\\&\quad+\pi p^2y_s^2-4\pi^3(\beta+g)^2y_H^2\ .\end{aligned}\tag{A2}$$

We note that the initial relation (2.7) and the initial form of the couplings $\alpha+g$, $\beta+g$, and $\alpha+\beta+2g$ in (A1) are all preserved under renormalization.

From the recursion for the y_H fugacity we find that the y_H is irrelevant for $\pi\alpha+\pi\beta>2$ when $g=0$ initially. However as $g<0$ hybrid vortices are relevant in the region where the two lines of Fig. 2 meet.

*Present address: Instituto de Befquisas Esbaciais, São José Dos Campos, Campos, S.P. 12200 Brazil.

[1] R. F. Voss and R. A. Webb, Phys. Rev. B 25, 3446 (1982); R. A. Webb, R. F. Voss, G. Grinstein, and P. M. Horn, Phys. Rev. Lett. 51, 690 (1983); S. Teitel and C. Jayaprakash, *ibid.* 51, 1999 (1983); Phys. Rev. B 27, 598 (1983).
[2] M. Y. Choi and S. Doniach, Phys. Rev. B 31, 4516 (1985).
[3] T. C. Halsey, J. Phys. C 18, 2437 (1985).
[4] S. Miyashita and H. Shiba, J. Phys. Soc. Jpn. 53, 1145 (1984); D. H. Lee, J. D. Joannopoulos, J. W. Negele, and D. P. Landau, Phys. Rev. Lett. 52, 433 (1984); Phys. Rev. B 33, 450 (1986).
[5] N. Parga and J. E. Himbergen, Solid State Commun. 35, 607 (1980).
[6] T. Garel and S. Doniach, J. Phys. C 13, L887 (1980).
[7] M. Yosefin and E. Domany, Phys. Rev. B 32, 1778 (1985); M. Y. Choi and D. Stroud, *ibid.* 32, 5773 (1985).
[8] B. Berge, H. T. Diep, A. Ghazali, and P. Lallemand (unpublished); E. Granato and J. M. Kosterlitz, J. Phys. C 19, L59 (1986).
[9] D. R. Nelson and B. I. Halperin, Phys. Rev. B 21, 5312 (1980).
[10] D. Mukamel, Phys. Rev. Lett. 34, 481 (1975).
[11] D. H. Lee and G. Grinstein, Phys. Rev. Lett. 55, 541 (1985).
[12] J. Villain, J. Phys. (Paris) 36, 581 (1975).
[13] L. P. Kadanoff, J. Phys. A 11, 1399 (1978).
[14] J. M. Kosterlitz and D. J. Thouless, J. Phys. C 6, 1181 (1973); J. M. Kosterlitz, *ibid.* 7, 1046 (1974).
[15] S. Elitzur, R. B. Pearson, and J. Shigemitsu, Phys. Rev. D 19,

3698 (1979).
[16]J. V. José, L. P. Kadanoff, S. Kirpatrick, and D. R. Nelson, Phys. Rev. B **16**, 1217 (1977).
[17]A. A. Migdal, Zh. Eksp. Teor. Fiz. **69**, 1457 (1975) [Sov. Phys.—JETP **42**, 743 (1976)].
[18]L. P. Kadanoff, Ann. Phys. (N.Y.) **100**, 359 (1976).
[19]M. B. Einhorn, R. Savit, and E. Rabinovici, Nucl. Phys. B **170**, 16 (1980).
[20]S. W. Heinekamp and R. A. Pelcovits, Phys. Rev. B **32**, 4528 (1985).
[21]R. H. Swendsen, Phys. Rev. B **17**, 3710 (1978).